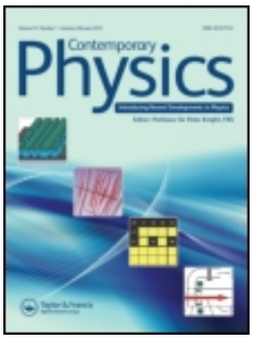

Contemporary Physics

ISSN: 0010-7514 (Print) 1366-5812 (Online) Journal homepage: www.tandfonline.com/journals/tcph20

The complex Ginzburg–Landau equation: an introduction

Vladimir García-Morales & Katharina Krischer

To cite this article: Vladimir García-Morales & Katharina Krischer (2012) The complex Ginzburg–Landau equation: an introduction, Contemporary Physics, 53:2, 79-95, DOI: 10.1080/00107514.2011.642554

To link to this article: https://doi.org/10.1080/00107514.2011.642554

Published online: 04 Jan 2012.

Contemporary Physics
Vol. 53, No. 2, March–April 2012, 79–95

Taylor & Francis
Taylor & Francis Group

The complex Ginzburg–Landau equation: an introduction

Vladimir García-Morales[a,b]* and Katharina Krischer[b]*

[a]*Institute of Advanced Study – TU München, Lichtenbergstr. 2a, D-85748 Garching, Germany;* [b]*Nonequilibrium Chemical Physics, Physik-Department, TU München, James-Franck-Str. 1, D-85748 Garching, Germany*

(*Received 9 August 2011; final version received 25 October 2011*)

The complex Ginzburg–Landau equation (CGLE), probably the most celebrated nonlinear equation in physics, describes generically the dynamics of oscillating, spatially extended systems close to the onset of oscillations. Using symmetry arguments, this article gives an easy access to this equation and an introduction into the rich spatio-temporal behaviour it describes. Starting out from the familiar linear oscillator, we first show how the generic model for an individual nonlinear oscillator, the so-called Stuart–Landau equation, can be derived from symmetry arguments. Then, we extend our symmetry considerations to spatially extended systems, arriving at the CGLE. A comparison of diffusively coupled linear and nonlinear oscillators makes apparent the source of instability in the latter systems. A concise survey of the most typical patterns in 1D and 2D is given. Finally, more recent extensions of the CGLE are discussed that comprise external, time-periodic forcing as well as nonlocal and global spatial coupling.

Keywords: nonlinear physics; spatially extended systems; oscillations; turbulence; resonant forcing; spatial coupling

1. Introduction

Oscillations are abundant in nature as well as in man-made systems and devices. When studying physics, one of the first concepts introduced is that of the linear, harmonic oscillator. It is appreciated that all systems exhibiting harmonic oscillations are governed by the same differential equation; only the interpretation of the equation's parameter, here the eigenfrequency of the system, changes. Nonlinear oscillators, which appear in all disciplines of natural sciences, are just as important as harmonic oscillations in linear physics. To name three examples, our life depends on stable oscillations of the heart; Josephson junctions, which are physical devices with large technological potential, generate voltage oscillations of an enormously high frequency; and concentrations of species during a chemical reaction might oscillate in time, as is the case in the famous Belousov–Zhabotinsky reaction. A decisive difference from linear oscillations is seen in their response to a small perturbation. When a linear oscillator is given a small 'kick', it simply oscillates with a different amplitude. In contrast, the amplitude of nonlinear oscillators is self-regulating: any perturbation away from the stable oscillation in phase space decays with time, the system relaxing back to the same region in phase space. Close to the onset of oscillations, also all nonlinear oscillators can be described by a universal mathematical model, the so-called Stuart–Landau equation, which is an ordinary differential equation of a complex order parameter.

The Stuart–Landau equation describes a single oscillator. Already from the examples mentioned above it becomes obvious that this description must be insufficient when dealing with a spatially extended system. Consider, for example, the Belousov–Zhabotinsky reaction carried out in a Petri dish where forced mixing of the solution is absent. Then, each small region – or point – in the Petri dish can be viewed as an oscillator, and the entire oscillating medium as being composed of infinitely many oscillators which are coupled by diffusion of the chemical species. As a result of the spatial coupling of the oscillators, a wealth of spatio-temporal patterns might form, ranging from regular plane waves to highly turbulent behaviour. An example of turbulent patterns which were observed during the catalytic CO oxidation on a Pt(110) surface are depicted in Figure 1.

When considering the two examples mentioned in the last paragraph, we see that the evolution equations governing the spatio-temporal dynamics of an oscillatory medium as obtained from physical laws can be cast in the form of a reaction diffusion (RD) equation

$$\frac{\partial \boldsymbol{y}}{\partial t} = \boldsymbol{f}(\boldsymbol{y}) + \mathbf{D}\nabla^2\boldsymbol{y}. \tag{1}$$

*Corresponding authors. Email: vmorales@ph.tum.de; krischer@ph.tum.de

ISSN 0010-7514 print/ISSN 1366-5812 online

http://dx.doi.org/10.1080/00107514.2011.642554
http://www.tandfonline.com

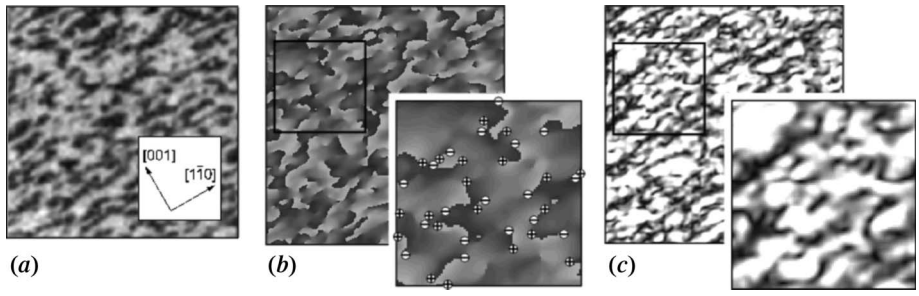

Figure 1. Chemical turbulence in catalytic CO oxidation on Pt(110). (*a*) PEEM image of size 275 × 275 μm^2. (*b*) Phase and (*c*) amplitude representations of (*a*) with zooms of selected regions indicated by rectangular boxes. The images are coded in a linear grey-scale colour table, where white (black) denotes high (low) values of the respective quantity. In the zoom in (*b*), the locations of topological defects are marked with the symbols + and −, according to their topological charge (taken from [1]). Reproduced figure with permission from C. Beta, A.S. Mikhailov, H.H. Rotermund, and G. Ertl, Europhys. Lett. 75 (2006), p. 868. Copyright (2006), IOP Publishing.

Here $\boldsymbol{y}$ is a vector containing the dynamical variables, $\boldsymbol{f}(\boldsymbol{y})$ is a (generally nonlinear) vector function of the dynamical variables, which describes the local oscillator, **D** is a diffusion matrix, often assumed to be diagonal, and the Laplacian on the r.h.s. acts on space. An RD equation contains many parameters that are specific to each system, as are the functions $\boldsymbol{f}(\boldsymbol{y})$. Hence, on this level of mathematical description, the possibility of making general predictions of pattern formation in oscillatory media is very limited. However, as Kuramoto [2] showed, all RD equations with a reaction dynamics close to the onset of oscillations, can be mapped to a universal model with a great predictive power, the complex Ginzburg–Landau equation (CGLE). Roughly speaking, one can say that the CGLE describes Stuart–Landau oscillators which are diffusively coupled.

In fact, the applicability of the CGLE goes far beyond RD systems. It was first derived by Newell and Whitehead in 1969 [3] when modelling the onset of instability in fluid convection problems. In these situations, at some critical value μ_c of a control parameter μ that can be tuned experimentally, a spatially homogeneous steady state loses stability to oscillations whose frequency ω_0 and wavelength can be understood in terms of a linearised equation. Newell and Whitehead found that when nonlinear effects are included, these oscillations are modulated over long time and space scales by a quantity W that plays a role of a complex order parameter. In fact, the complex Ginzburg–Landau equation arises generically in fluid dynamics, as shown by Stewartson and Stuart in 1971 in the context of plane Poiseuille flow [4]. A number of reviews and important works have appeared during the last two decades, showing the generality of the CGLE in many physical situations at all scales [5–10]. Introductory works to the subject can also be found in [11–15].

The goal of this article is to give a concise and easily accessible 'primer' to the CGLE which should bring the reader to the state of being able to understand original research papers. In the next section, starting from the simple harmonic oscillator we derive the Stuart–Landau equation (SLE) from symmetry arguments. The SLE describes in general *one* nonlinear oscillator, or a spatially extended system like in Equation (1) when coupled so strongly that the entire medium oscillates in synchrony. Then, we add diffusion to our considerations, again first to a linear oscillator and then to the SLE. We thus arrive at the CGLE which corresponds to a spatially extended field of Stuart–Landau oscillators which are coupled through diffusion. In the third part we discuss the basic solution of the CGLE in 1D and 2D. The last two sections consider two extensions of the CGLE, namely external resonant forcing of the oscillator and nonlocal spatial coupling. It is the aim of this paper to show how symmetry reasoning allows us to understand both the SLE and the CGLE, as well as its extensions, in a general way.

2. The linear harmonic oscillator and the rotation symmetry in the complex plane

As already mentioned, the harmonic oscillator is a universal model for many systems in nature when they are subject to oscillations of small amplitude. The ones in Figure 2 are well known examples: a simple pendulum, a spring with low elongation, an *LC* electrical circuit. The universality of such a mathematical model, and the quantities involved in it, such as amplitude and frequency of the oscillations, take specific forms depending on the physical system under consideration. So, for a simple mathematical pendulum, the angular frequency ω_0 is given by $(g/\ell)^{1/2}$, where ℓ is the pendulum's length and g is the constant of gravity; for a spring, the frequency is given by $(k/m)^{1/2}$, where k is the spring's constant and m the mass attached to it; while for an *LC* circuit the frequency is given by $(1/LC)^{1/2}$, where L and C are the inductance and the

capacitance, respectively. Mathematical considerations of a general model such as the simple harmonic oscillator thus elucidate the dynamical behaviour of a wide variety of systems which can be mapped to such a class of model. In general, the dynamics of a linear harmonic oscillator of amplitude R, phase ϕ and angular frequency ω_0 can be described in polar coordinates as

$$\dot{R} = 0,$$
$$\dot{\phi} = \omega_0. \tag{2}$$

These two equations can easily be integrated to give $R = R_0$ and $\phi = \omega_0 t + \phi_0$, where R_0 and ϕ_0 are integration constants specifying the initial amplitude and phase of the oscillations, respectively. If we define the complex valued quantity $W = |W| \exp(\mathrm{i}\phi) \equiv R \exp(\mathrm{i}\phi)$ we can write Equations (2) as

$$\dot{W} = \mathrm{i}\omega_0 W. \tag{3}$$

Taking the time derivative of both sides of the latter equation and using it to replace $\dot{W}$, we obtain the second-order differential equation for the simple harmonic oscillator $\ddot{W} = -\omega_0^2 W$. It is clear that Equation (3) is rotationally invariant, i.e. if χ is an arbitrary real number, then the change

$$W \rightarrow W \exp(\mathrm{i}\chi) \tag{4}$$

leaves Equation (3) unchanged.

We can understand this rotation symmetry in the complex plane by looking at the dynamics of the linear harmonic oscillator more closely. The Hamiltonian H of the latter can be written generally as

$$H = \frac{p^2}{2m} + \frac{1}{2} m\omega_0^2 q^2 = E, \tag{5}$$

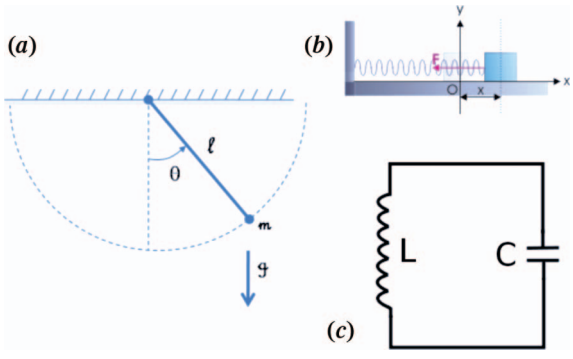

Figure 2. Examples of systems well described by the simple harmonic oscillator: (*a*) mathematical pendulum; (*b*) spring under small elongation; (*c*) an LC electrical circuit.

where q and p denote the position and momentum coordinates, respectively, and m is the mass. The total energy E of the system is conserved and equal to the Hamiltonian. The trajectories in the phase plane, specified by the pair (q, p), can be directly plotted from Equation (5) and correspond to concentric ellipses. We can rescale the Hamiltonian by introducing the changes $q \rightarrow q/m^{1/2}$ and $p \rightarrow m^{1/2}p$, so that it reads as a linear harmonic oscillator with unit mass

$$H = \frac{p^2}{2} + \frac{1}{2}\omega_0^2 q^2 = E. \tag{6}$$

It is now to be noted that this equation specifies concentric circles in the plane $(\omega_0 q, p)$ with radius $(2E)^{1/2}$ (see Figure 3 where the loci of two different trajectories are plotted for two different values of the energy, $E_2 > E_1$). The equations of motion are then given by

$$\dot{q} = \frac{\partial H}{\partial p} = p, \tag{7}$$

$$\dot{p} = -\frac{\partial H}{\partial q} = -\omega_0^2 q. \tag{8}$$

It is clear from these equations and from Figure 3, that when $|q|$ increases $|p|$ decreases and, conversely, when $|q|$ decreases, $|p|$ increases. On the phase plane, we can define now the complex amplitude $W = \omega_0 q - \mathrm{i}p = (\omega_0^2 q^2 + p^2)^{1/2} \exp(\mathrm{i}\phi) = (2E)^{1/2} \exp(\mathrm{i}\phi)$ with $\phi = \arctan(-p/\omega_0 q)$. W moves on concentric circumferences of radius $(2E)^{1/2}$. We then recover Equation (3)

$$\dot{W} = \omega_0 \dot{q} - \mathrm{i}\dot{p} = \omega_0 p + \mathrm{i}\omega_0^2 q = \mathrm{i}\omega_0(\omega_0 q - \mathrm{i}p) = \mathrm{i}\omega_0 W, \tag{9}$$

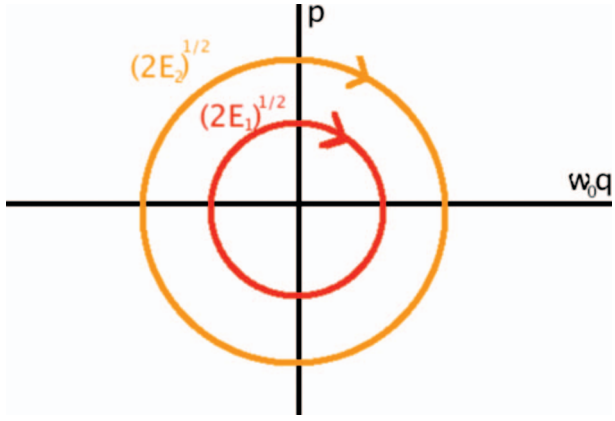

Figure 3. Trajectories of the harmonic oscillator on phase space specified by the coordinates $(\omega_0 q, p)$ for two different values of the energy E, $E_2 > E_1$.

The rotation symmetry, Equation (4), makes explicit the symmetry of the trajectories on the phase plane: there is no possible distinction of the system's physical behaviour at different phases ϕ regarding energy. This is a fundamental symmetry property of the linear harmonic oscillator: the energy of the harmonic oscillator depends only on the square of the amplitude of the oscillations (i.e. on $|W|^2$), but not on the phase. There are no *privileged* phases in the system.

3. Introducing the simplest nonlinearity preserving the rotation symmetry: the Stuart–Landau Equation (SLE)

Considering small amplitude oscillations, we can now ask what would be the lower nonlinear corrections to Equation (3) in the amplitude W, while preserving the phase invariance, Equation (4). Preserving this invariance is important not only when the energy E is conserved: all autonomous oscillations are invariant with respect to rotation in phase since none of the phases is preferred over another one. Since the square of the modulus of the amplitude is given by $|W|^2 = WW^*$ we can consider a function $f(W,W^*)$ modifying Equation (3) so that

$$\dot{W} = \mathrm{i}\omega_0 W + f(W, W^*). \tag{10}$$

Now, it is clear that under the transformation $W \to W\exp(\mathrm{i}\chi)$ $(W^* \to W^*\exp(-\mathrm{i}\chi))$ the function $f(W,\ W^*)$ has to satisfy $f(W\exp(\mathrm{i}\chi),\ W^*\exp(-\mathrm{i}\chi)) = f(W,\ W^*)\exp(\mathrm{i}\chi)$ so that the exponential factor containing the phase χ can be factored out in Equation (10). If we expand $f(W,W^*)$ in powers of W and W^* (small amplitude oscillations) we find that to the lowest order of the nonlinearity, in order to satisfy phase invariance we must have

$$f(W, W^*) = \alpha_1 W + \alpha_2 |W|^2 W, \tag{11}$$

where both $\alpha_1 = \alpha_{1r} + \mathrm{i}\alpha_{1i}$ and $\alpha_2 = \alpha_{2r} + \mathrm{i}\alpha_{2i}$ are complex numbers. By replacing this form of $f(W,W^*)$ in Equation (10) and switching again to polar coordinates $W = R\exp(\mathrm{i}\phi)$ we find

$$\begin{aligned} \dot{R} &= \alpha_{1r} R + \alpha_{2r} R^3, \\ \dot{\phi} &= \omega_0 + \alpha_{1i} + \alpha_{2i} R^2. \end{aligned} \tag{12}$$

We can now pass to the reference frame rotating with the frequency of the unmodified linear oscillator by setting $\phi = \varphi + \omega_0 t$

$$\begin{aligned} \dot{R} &= \alpha_{1r} R + \alpha_{2r} R^3, \\ \dot{\varphi} &= \alpha_{1i} + \alpha_{2i} R^2. \end{aligned} \tag{13}$$

The r.h.s. of these equations describe the modification to the dynamics of the linear oscillator introduced by the nonlinear function $f(W,W^*)$ in Equation (10). If we think of the parameters α_1 and α_2 as some quantities that can be switched on to have a finite nonvanishing value, we see that *the nonlinearity will drive the linear oscillator from an amplitude R_0 as we obtained from Equation (2) to a stationary value of the amplitude $R^{(\mathrm{st})}$ that can be either 0 or* $(-\alpha_{1r}/\alpha_{2r})^{1/2}$. These values are obtained by setting $\dot{R} = 0$ in Equations (13). To have sustained oscillations under the effect of the nonlinearity we therefore require that the state with $R^{(\mathrm{st})} = (-\alpha_{1r}/\alpha_{2r})^{1/2}$ exists and is stable. The existence of this state is guaranteed if α_{1r} and α_{2r} have opposite signs. The stability requires that any perturbation u around this state $R = R^{(\mathrm{st})} + u$ does not grow with time. The dynamics of the perturbation is given from Equation (13) by

$$\dot{u} = (\alpha_{1r} + 3\alpha_{2r} R^{(\mathrm{st})2})u = -2\alpha_{1r} u \tag{14}$$

and this implies that the state with stationary nonvanishing amplitude will be stable if $\alpha_{1r} > 0$ since in such a case any perturbation will decay exponentially. Therefore, we pick $\alpha_{2r} < 0$. The stability of the state $R^{(\mathrm{st})} = 0$ is the opposite and requires $\alpha_{1r} < 0$. Exactly at $\alpha_{1r} = 0$ we have a linear oscillator if we neglect the cubic and the quadratic terms in Equation (13). In the rest of this paper we will work in a limit where the character of the nonlinearity, which, as can be understood from the preceding analysis, is switched on by α_{1r}, is weak. We introduce then the small parameter μ and define $\alpha_{1r} \equiv \mu\sigma_1$ (with $\sigma_1 > 0$) and $\alpha_{1i} \equiv \mu\omega_1$. Since $\alpha_{2r} < 0$ we also define $\alpha_{2r} \equiv -g_r$ $(g_r > 0)$ and $\alpha_{2i} \equiv -g_i$ (which can be either positive or negative). With all these redefinitions, Equations (13) now read

$$\begin{aligned} \dot{R} &= \mu\sigma_1 R - g_r R^3, \\ \dot{\varphi} &= \mu\omega_1 - g_i R^2. \end{aligned} \tag{15}$$

Starting from a state with a vanishingly small amplitude R, it will grow exponentially as $\sim\exp(\mu\sigma_1 t)$, but then it will saturate at a value $(\mu\sigma_1/g_r)^{1/2}$ owing to the presence of the cubic term. The parameter g_i controls the strength of the nonlinear effects of the amplitude on the frequency of the oscillations. If we switch again to the complex plane $R\exp(\mathrm{i}\varphi) \to W$, we finally have

$$\dot{W} = \mu(\sigma_1 + \mathrm{i}\omega_1)W - (g_r + \mathrm{i}g_i)|W|^2 W. \tag{16}$$

This is the so-called Stuart–Landau equation, which constitutes a universal model for oscillators with a weak nonlinearity. For $\mu = 0$, $g_r = 0$ and $g_i = 0$ the linear oscillator of frequency ω_0 is recovered (in a

rotating reference frame moving with the frequency of the oscillator so that $\dot{W} = 0$). When $\mu < 0$ the oscillations are damped and $W \to 0$ as $t \to \infty$, and when $\mu > 0$, the system is driven to regular oscillations with an absolute value of the complex amplitude $|W| = (\mu\sigma_1/g_r)^{1/2}$ and frequency $\omega_0 + \mu(\omega_1 - g_i\sigma_1/g_r)$. Hence, when μ crosses zero, the dynamics changes from a stable fixed point (and no sustained oscillations) to a stable oscillatory regime. This scenario corresponds to what is called a supercritical Hopf bifurcation (see Figure 4). The Stuart–Landau equation is a universal model for oscillators close to this bifurcation. Looking again at Equation (15) we can get some insight into the meaning of the parameters. In the oscillatory region, $\mu\sigma_1$ is the characteristic rate with which the oscillation amplitude grows from the unstable fixed point. This growth is the slower the closer we are to the Hopf bifurcation. Also the departure of the frequency of the oscillation from the eigenfrequency of the underlying linear oscillator at $\mu = 0$ increases with the distance to the Hopf bifurcation and with the amplitude of the oscillator.

As a specific example, let us consider the dynamics given by $\boldsymbol{y} = (y_1, y_2)$ as

$$\begin{aligned} \dot{y}_1 &= -y_2 + y_1[\mu - (y_1^2 + y_2^2)], \\ \dot{y}_2 &= y_1 + y_2[\mu - (y_1^2 + y_2^2)]. \end{aligned} \tag{17}$$

Introducing the polar coordinates (r,θ) so that

$$\begin{aligned} y_1 &= r\cos\theta, \\ y_2 &= r\sin\theta, \end{aligned} \tag{18}$$

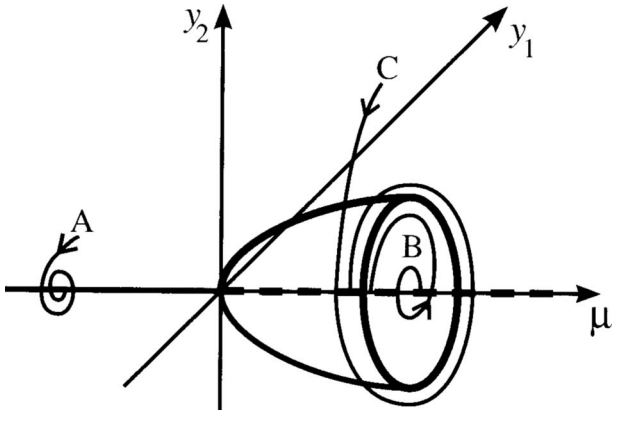

Figure 4. Supercritical Hopf bifurcation. For $\mu < 0$, the steady state (0,0) (on the μ axis) is stable and the trajectory of a neighbouring point A is a stable spiral. For $\mu > 0$ the state (0,0) is no longer stable and a neighbouring point B develops an unstable spiral converging to a limit cycle. The same applies to a point C far away from the stationary state. The limit cycle is an attractor for all trajectories when $\mu > 0$.

the dynamics can be written, after some algebra, as

$$\begin{aligned} \dot{r} &= r[\mu - r^2], \\ \dot{\theta} &= 1, \end{aligned} \tag{19}$$

which has clearly the form of Equations (15) with $\sigma_1 = g_r = 1$, $\omega_1 = 1/\mu$ and $g_i = 0$. The system has clearly a supercritical Hopf bifurcation at $\mu = 0$. In this specific case, the frequency depends neither on the distance to the Hopf bifurcation nor on the amplitude.

4. Spatially extended systems: the complex Ginzburg–Landau equation

Let us now consider a spatially extended system, where at each point x there is a physical property that presents oscillations, say concentrations of chemical species. In the following, we will confine our discussion to 1D systems for simplicity. The complex amplitude $W(x,t)$ at each point can be thought to represent in a general way the dynamical state of the system. Let us first consider a case where the local dynamics corresponds to simple (linear) harmonic oscillators. When there exist spatial heterogeneities in the complex amplitude, diffusion will work to homogenise the system, both in the absolute value and in its phase. We can see this if we add a diffusion term to Equation (3)

$$\partial_t W = \mathrm{i}\omega_0 W + D\partial_x^2 W, \tag{20}$$

where $D = d_r + \mathrm{i}d_i$ is a complex constant and we have now a partial differential equation because of both the time and spatial dependence of W. The meaning of the complex diffusion coefficient should be clear if we think that the complex order parameter $W(x,t)$ contains information both on the (real) amplitude and the (real) phase of an oscillatory physical quantity. Diffusion tends to homogenise spatial gradients of such an oscillatory quantity. If we think that at a given point x the concentration of a chemical oscillates in time and that the oscillatory state is fully described by the complex order parameter $W(x,t)$, diffusion will work so as to smooth any spatial gradient in phase and amplitude. Otherwise, there would always exist a gradient in chemical concentrations when $|W(x,t)| = |W(x',t)|$ but $\phi(x,t) \neq \phi(x',t)$, or when $\phi(x,t) = \phi(x',t)$ but $|W(x,t)| \neq |W(x',t)|$. The complex diffusion coefficient can be derived from the physical diffusion coefficient (a real quantity) through a one to one correspondence when one passes to the reference frame of the oscillatory complex quantity $W(x,t)$.

When all points have the same value of W (the homogeneous situation) the whole spatial system oscillates synchronously and Equation (3) represents both, the oscillatory behaviour at each point in space and the 'bulk' collective oscillation (since the distribution of the complex amplitude is homogeneous, the diffusion term vanishes in Equation (20)). For further analysis, and without loss of generality, let us consider a ring of length L as the spatial geometry. It is clear then that the complex amplitude must satisfy $W(x,t) = W(x + L,t)$ and any solution should satisfy this requirement. Hence, we can expand the general solution for the complex amplitude in Fourier series in the following way

$$W(x,t) = \sum_{n=-\infty}^{+\infty} W_n(t) \exp(\mathrm{i}2\pi n x/L), \tag{21}$$

which clearly is invariant upon a translation $x \to x + L$. The mode $n = 0$ corresponds to the homogeneous situation. Each Fourier mode corresponds to a different solution periodic in space with wavenumber $q = 2\pi n/L$. The time evolution of its complex amplitude can be calculated if we insert Equation (21) into Equation (20). Then, we obtain the evolution equations of the amplitude of the mode n

$$\partial_t W_n = \mathrm{i}\omega_0 W_n - \left(\frac{2\pi n}{L}\right)^2 D W_n, \tag{22}$$

which can be readily integrated to give

$$W_n(t) = W_n(0) \exp\left[-\left(\frac{2\pi n}{L}\right)^2 d_r t\right] \exp(\mathrm{i}\omega_n t), \tag{23}$$

where $\omega_n = \omega_0 - (2\pi n/L)^2 d_i$. All Fourier modes with $n \neq 0$ will be damped and, in the long time limit, only the homogeneous mode, corresponding to bulk oscillations with frequency ω_0, will survive in the general solution of Equation (20). Fourier modes with shorter wavelengths, i.e. with n large, are more strongly damped than those with n small.

Let us now turn to Stuart–Landau oscillators, adding a diffusion term. Equation (16) is then modified as

$$\partial_t W = \mu(\sigma_1 + \mathrm{i}\omega_1) W - (g_r + \mathrm{i}g_i)|W|^2 W + (d_r + \mathrm{i}d_i)\partial_x^2 W, \tag{24}$$

where $D = (d_r + \mathrm{i}d_i)$ is the complex diffusion coefficient. Equation (24) is the Complex Ginzburg–Landau equation. If we consider a situation where we can neglect the cubic term (small amplitude W) and we insert Equation (21) in Equation (24) we have

$$\partial_t W_n \approx \left[\mu\sigma_1 - \left(\frac{2\pi n}{L}\right)^2 d_r + \mathrm{i}\left(\omega_1 - \left(\frac{2\pi n}{L}\right)^2 d_i\right)\right] W_n, \tag{25}$$

which can be integrated (being an approximation for all times at which W_n remains small) as

$$W_n(t) = W_n(0) \exp\left[\left(\mu\sigma_1 - \left(\frac{2\pi n}{L}\right)^2 d_r\right) t\right] \exp(\mathrm{i}\omega_n t), \tag{26}$$

where $\omega_n = \omega_1 - (2\pi n/L)^2 d_i$. Since μ and σ_1 are positive, it is clear that the homogeneous mode $n = 0$ will grow exponentially until the cubic term in Equation (24) becomes relevant. Other Fourier modes with $n \neq 0$ relevant to the dynamics in the long time limit will be those for which

$$\mu\sigma_1 - \left(\frac{2\pi n}{L}\right)^2 d_r > 0. \tag{27}$$

For sufficiently large system length L there will be a band of Fourier modes with long wavelengths which satisfy this inequality. These modes will grow exponentially and exchange energy until the cubic term makes them saturate. Yet this requires further analysis since the behaviour of the cubic term couples the Fourier modes in a complicated way and spatiotemporal pattern formation can take place where combinations of Fourier modes become active in the pattern, breaking certain symmetries. This is the interesting fact about amplitude equations: its close relationship with dynamical orders, specified by the groups of Fourier modes that become active in pattern formation. For sufficiently high n, however, the latter inequality will not hold and the Fourier modes will be damped as in Equation (26). In the limit $L \to 0$, the Stuart–Landau equation is recovered, since only the homogeneous mode will be able to grow, the mode with $n = 1$ already violating the inequality Equation (27). Note that L^2/d_r is the time a species with diffusion coefficient d_r needs to propagate over a distance L. Thus, Equation (27) compares the characteristic reaction and diffusion times. When $\mu\sigma_1 L^2/d_r \gg 1$ a thick band of relevant Fourier modes with long wavelengths will be significant to the dynamics. The latter slowly modulate the homogeneous profile. The reaction time becomes smaller as we depart from the Hopf bifurcation and the diffusion time decreases as the system length is increased.

Assuming that μ is positive (i.e. that we are in the oscillatory regime) we can cast Equation (24) in a more

elegant way. When scaling time to the characteristic reaction time, space to the characteristic diffusion length (corresponding to the reaction time) and the modulus of the amplitude to the radius of the limit cycle, i.e. introducing the following transformations

$$t \to \frac{t}{\mu\sigma_1} \quad x \to \left(\frac{d_r}{\mu\sigma_1}\right)^{1/2} x$$
$$W \to \left(\frac{\mu\sigma_1}{g_r}\right)^{1/2} \exp(\mathrm{i}\omega_1 t/\sigma_1) W \tag{28}$$

and defining

$$c_1 = \frac{d_i}{d_r} \quad c_2 = \frac{g_i}{g_r} \tag{29}$$

Equation (24) becomes

$$\partial_t W = W - (1 + \mathrm{i}c_2)|W|^2 W + (1 + \mathrm{i}c_1)\partial_x^2 W, \tag{30}$$

where we also moved to a frame rotating with ω_1/σ_1. In this form, the parameter μ is scaled out and, besides the system length L only two parameters, c_1 and c_2, are present. The latter may be calculated by the nonlinear function of the homogeneous dynamics $\boldsymbol{f}(\boldsymbol{y})$ in Equation (1). The advantage of this equation is its generality: regardless of the number of parameters and scalar equations contained in Equation (1), the dynamics is universal at the onset of oscillatory behaviour and can be mapped onto the CGLE Equation (30). Only two parameters c_1 and c_2 lump together all the parameters entering in the homogeneous dynamics and the diffusion term in Equation (1) and are essential to describe the universal dynamics close to the bifurcation.

At the onset of oscillatory behaviour, one can expand the solution $\boldsymbol{y}$ of the general reaction-diffusion system Equation (1) in powers of $(\mu - \mu_c)^{1/2}$. We assume for simplicity, but without lack of generality, that $\mu_c = 0$ in all the following. The solution $\boldsymbol{y}$ to order zero in $\mu^{1/2}$ gives the location of the fixed-point. At order $\mu^{1/2}$ the solution behaves as an harmonic oscillation that is a linear combination of the order parameter W and its complex conjugate W^* which depends both on a slow time scale $\sim\mu^{1/2}t$ and a slow spatial scale $\sim\mu^{1/2}x$ i.e.

$$W(\mu^{1/2}t, \mu^{1/2}x)\exp(\mathrm{i}\omega_0 t) + W^*(\mu^{1/2}t, \mu^{1/2}x)\exp(-\mathrm{i}\omega_0 t). \tag{31}$$

At order μ, the solution $\boldsymbol{y}$ is also oscillatory and depends on the second harmonic of the base oscillation and contains terms $\propto W^2\exp(2\mathrm{i}\omega_0 t)$, $\propto W^{*2}\exp(-2\mathrm{i}\omega_0 t)$ and $|W|^2$. Thus, the solution of the CGLE, Equation (30), gives the dependence of the order parameter W (and hence of its complex conjugate as well) on x and t.

5. Solutions of the CGLE. Linear stability analysis of the uniform oscillation

The CGLE has plane waves as specific solutions

$$W_Q = a_Q \exp[\mathrm{i}(\omega_Q t + Qx)] \tag{32}$$

with

$$|a_Q|^2 \equiv 1 - Q^2, \tag{33}$$

$$\omega_Q \equiv -c_2 + (c_2 - c_1)Q^2, \tag{34}$$

where Q is the wavenumber of the plane wave. This can be easily checked by substituting Equation (32) into Equation (30). Plane waves are stable over wide parameter ranges in the $c_1 - c_2$ parameter space. There are also regions of *multistability*, where a certain number of plane waves are, each of them individually, stable. In such situations, the stationary state that is reached depends on the initial condition.

The stability of the uniform oscillation ($Q = 0$, $|a_0| = 1$, $\omega_0 = -c_2$) can be studied by perturbing the CGLE [2]. Inserting $W \approx [1 + w(x,t)]\exp(\mathrm{i}\omega_0 t)$ in Equation (30), and neglecting terms in the perturbation $\sim ww$, $\sim ww^*$, $\sim w^*w^*$ (the asterisk denotes complex conjugation) from second order on, we obtain

$$\partial_t w = -(1 + \mathrm{i}c_2)[w + w^*] + (1 + \mathrm{i}c_1)\partial_x^2 w. \tag{35}$$

If we carry the Fourier transform of the latter equation in the spatial dimension, we obtain, for the mode with wavenumber $q = 2\pi n/L$, again assuming periodic boundary conditions, we get

$$\partial_t w_q = -(1 + \mathrm{i}c_2)[w_q + w_q^*] - (1 + \mathrm{i}c_1)q^2 w_q, \tag{36}$$

where w_q and w_q^* are the Fourier transforms of w and $w*$, respectively. By taking the complex conjugate of Equation (36) we obtain

$$\partial_t w_q^* = -(1 - \mathrm{i}c_2)[w_q + w_q^*] - (1 - \mathrm{i}c_1)q^2 w_q^*. \tag{37}$$

We can write Equations (36) and (37) in matrix form as

$$\partial_t \begin{pmatrix} w_q \\ w_q^* \end{pmatrix} = \begin{pmatrix} -(1 + \mathrm{i}c_2) - (1 + \mathrm{i}c_1)q^2 & -(1 + \mathrm{i}c_2) \\ -(1 - \mathrm{i}c_2) & -(1 - \mathrm{i}c_2) - (1 - \mathrm{i}c_1)q^2 \end{pmatrix} \begin{pmatrix} w_q \\ w_q^* \end{pmatrix}. \tag{38}$$

The diagonalisation of the matrix on the r.h.s. yields a quadratic characteristic equation whose solution are the eigenvalues

$$\lambda_{\pm}^{(q)} = -(1+q^2) \times \left\{ 1 \pm \left(1 - \frac{q^2\left[(1+c_1^2)q^2 + 2(1+c_1c_2)\right]}{(1+q^2)} \right)^{1/2} \right\}. \quad (39)$$

When both eigenvalues are negative, for all Fourier modes any perturbation w is damped exponentially and the uniform oscillation is stable. When, however, any of the eigenvalues is positive for some q, the perturbations w_q, w_q^* grow exponentially and a pattern emerges formed by inhomogeneities corresponding to such Fourier modes. (It is to be noted that the perturbations cannot grow indefinitely because of the nonlinear term in the CGLE.) The uniform oscillation then becomes unstable in such cases. Hence, to have an instability, the following condition then needs to be satisfied

$$1 + c_1c_2 < 0. \quad (40)$$

Otherwise, both eigenvalues in Equation (39) are negative. When, however, the latter condition holds, a band of unstable wavenumbers emerges and destabilises the uniform oscillation. Using Equation (39) we see that this band lies in the range

$$0 < |q| < \left(\frac{2|1+c_1c_2|}{1+c_1^2} \right)^{1/2}. \quad (41)$$

The curve $1 + c_1c_2 = 0$ in the $c_1 - c_2$ parameter plane is the so-called Benjamin–Feir line and marks the border between regions where the uniform oscillation is linearly stable and unstable. The patterns that emerge in the unstable region are very interesting and justify the status of the CGLE in studying complex behaviour.

In Figure 5, the spatiotemporal evolution of the absolute value $|W|$ of the complex amplitude and of the phase are plotted in a situation where $1 + c_1c_2 \lesssim 0$, i.e. where the instability is weak and only long wavenumbers are present, as given by Equation (41). We observe that, while $|W| \approx 1$ for almost all times and spatial locations, the phase experiences modulations that are turbulent: the uniform oscillation is destabilised and although the order parameter oscillates at each point in a manner that resembles the uniform oscillation (since the amplitude is almost uniform), the oscillators are no longer in phase. This situation is called *phase turbulence*.

In Figure 6, the spatiotemporal evolution of $|W|$ and of the phase are plotted for a situation deeper in the unstable regime, i.e. $1 + c_1c_2 \ll 0$. Now, the amplitude is distributed very inhomogeneously and can even vanish at certain points. When this happens, a jump in the phase occurs. The spatial distribution of the phase is discontinuous since there are points where the amplitude goes to zero, the phase no longer being defined. This can be understood from the definition of the phase ϕ

$$\tan\phi = \frac{\mathrm{Im}\, W(x,t)}{\mathrm{Re}\, W(x,t)}, \quad (42)$$

where Im W and Re W denote the imaginary and the real parts of the amplitude, respectively. When a defect occurs at a point x_0 at a given time t, both

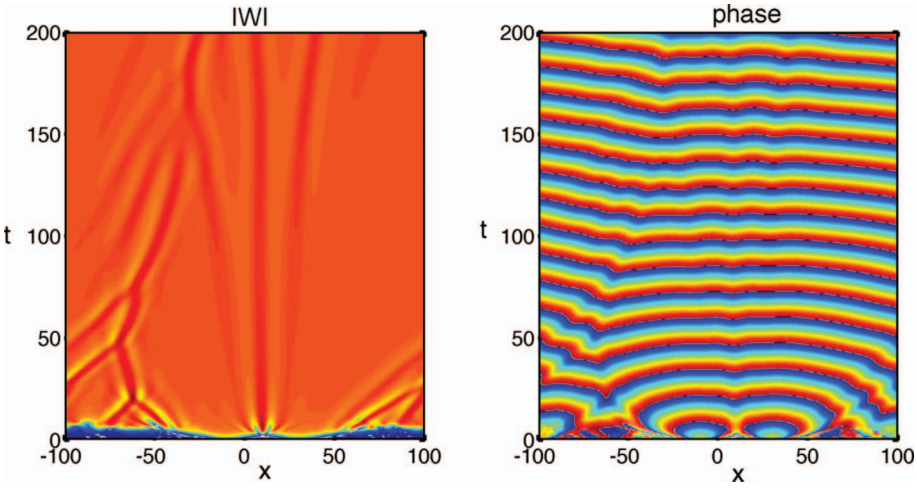

Figure 5. Spatiotemporal evolution of the absolute value $|W|$ of the complex amplitude (left) and phase (right) in a situation of phase turbulence: $c_1 = -4$, $c_2 = 0.5$.

Im $W = 0$ and $Re\ W = 0$ and we have, furthermore, in general

$$\lim_{x \to x_0^+} \frac{\text{Im } W(x,t)}{\text{Re } W(x,t)} \neq \lim_{x \to x_0^-} \frac{\text{Im } W(x,t)}{\text{Re } W(x,t)}. \qquad (43)$$

Since the limits approaching x_0 from the right and from the left do not coincide on a defect, the phase experiences a discontinuity, and the lines of constant phase are broken. These discontinuities can be clearly seen in Figure 6 (right) as open ends of constant phase lines. This kind of turbulent behaviour is called *defect turbulence* and contrasts with the above described phase turbulence. In the latter there are no discontinuities in the phase since $W(x,t) \approx 1$ for all x and t and the phase is therefore a continuous and well-defined function at every point.

Although the above linear stability analysis of the uniform oscillation gives a necessary condition for stability, there may be other stable plane wave solutions and chaotic behaviour may be also found even when $1 + c_1 c_2 > 0$ over broad regions in parameter space. In Figure 7 a situation of so-called *spatiotemporal chaos* [16] is shown for parameter values where the linear stability analysis predicts indeed that the uniform solution is *stable*. Broad regions of high amplitude of triangular shape are

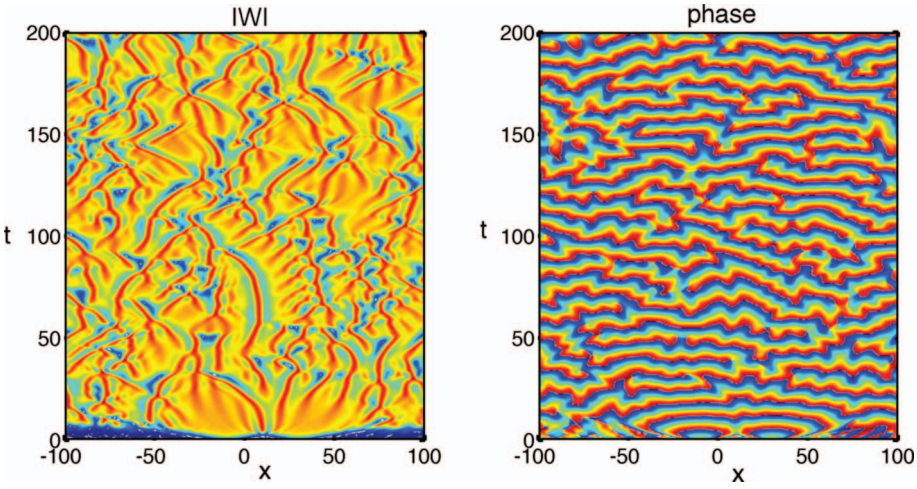

Figure 6. Spatiotemporal evolution of the absolute value $|W|$ of the complex amplitude (left) and phase (right) in a situation of defect turbulence: $c_1 = -4$, $c_2 = 1$.

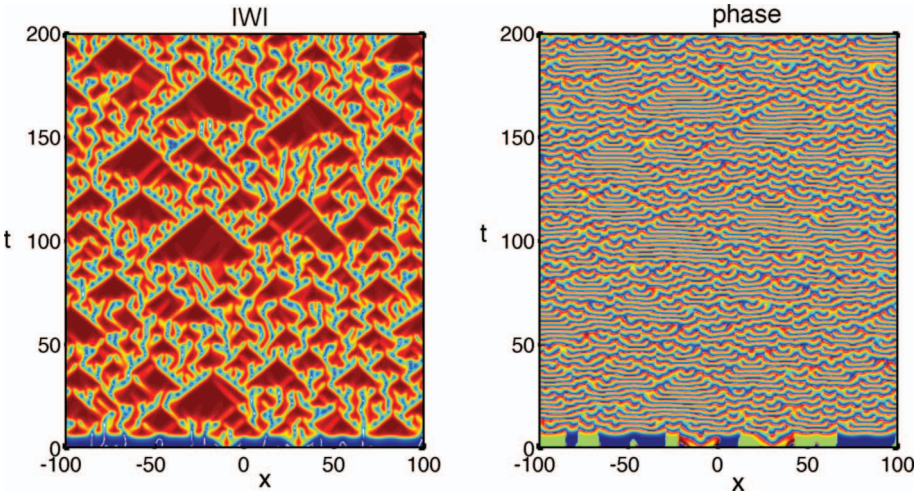

Figure 7. Spatiotemporal evolution of the absolute value $|W|$ of the complex amplitude (left) and phase (right) in a situation of spatiotemporal chaos: $c_1 = 0$, $c_2 = -3$.

irregularly interrupted by regions which are rich in amplitude defects.

In all the above description we have always discussed the one-dimensional CGLE. Of course, the results can be extended to two and three spatial dimensions. There, also defect turbulence and spatiotemporal chaos are present. In Figure 8 we show for a rectangular domain (periodic boundary conditions are considered) and for parameter values $c_1 = 0$ and $c_2 = 1$ the spatial distribution of $|W|$ and phase on the rectangle after a long iteration time. Twelve defects are observed on an, otherwise, homogeneous background of high amplitude. The defects determine centres of spirals, where the continuity of the phase distribution is broken, analogously to the 1D case. Each defect is characterised by a topological charge, which corresponds to the circulation of the gradient of the phase on a closed contour that contains the defect

$$m_{\text{top}} = \frac{1}{2\pi} \oint \nabla \phi(r, t) \cdot \mathrm{d}s. \tag{44}$$

Defects of this kind arise frequently in experiments, such as the ones we mentioned in the introduction (see Figure 1(*b*)). Note that in 2D defects persist in time while space–time defects in 1D exist only at a particular instant in time.

Prominent examples of physical experimental systems to which the CGLE has been applied are hydrodynamic systems such as electroconvection in nematic liquid crystals or Rayleigh–Benard systems [17]. The CGLE was also used in other fields, e.g. to study the transition from spirals to defect turbulence driven by a convective instability in the chemical Belousov–Zhabotinsky reaction [18] or, in biology, to model chaotic spirals observed during the chaotic aggregation of Dictyostelium [19].

6. Breaking phase invariance through an external resonant forcing

As in the case of a linear oscillator, the need to understand the response of a nonlinear oscillator to an external time-periodic driving force is relevant to many physical situations. This problem is considered in the following section where we again start our approach with symmetry arguments.

The phase invariance possessed by the CGLE can be interpreted as a continuum time translation symmetry. Since the system oscillates periodically with (roughly) the main base frequency ω_0 and all other oscillating terms can be considered as modulations of this trend on a long time scale, a phase shift transformation Equation (4), can be interpreted as a displacement in time, with respect to the dynamical behaviour at a given instant t_0. Let us consider, for simplicity a state where the uniform oscillation is stable (for other patterns formed by combinations of Fourier modes in time the same considerations apply). We can introduce a time shift transformation as

$$\begin{aligned} &W \equiv W_0 \exp(\mathrm{i}\omega_0 t) \rightarrow W_0 \exp[\mathrm{i}\omega_0 (t + t_0)], \\ &W \rightarrow W \exp(\mathrm{i}\omega_0 t_0), \end{aligned} \tag{45}$$

which is clearly the same as in Equation (4), $W \rightarrow W\exp(\mathrm{i}\chi)$ with $\chi = \omega_0 t_0$. When an external resonant forcing is introduced [20], i.e. when an external

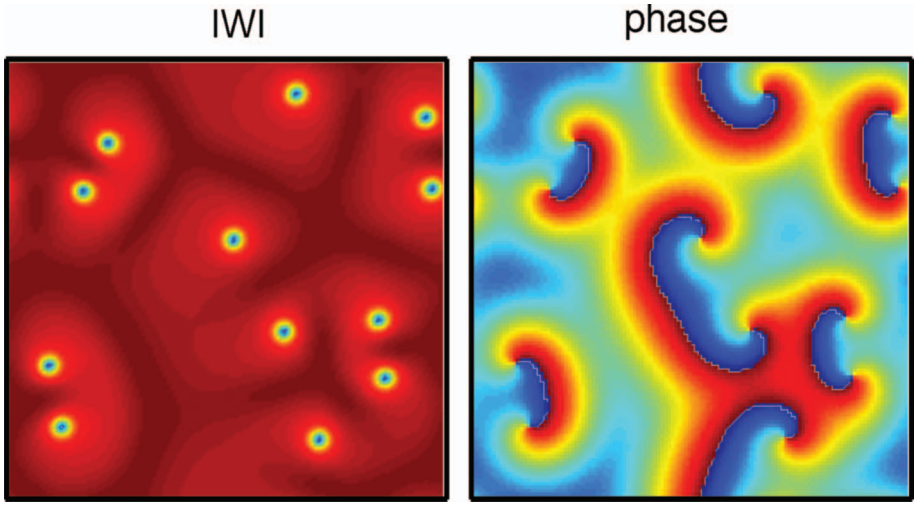

Figure 8. Spatial distribution of the absolute value $|W|$ of the complex amplitude (left) and phase (right) obtained after a transient from the 2D CGLE on a rectangular domain of 76 × 76 size in a situation of spatiotemporal chaos: $c_1 = 0$, $c_2 = 1$.

oscillatory signal with a frequency commensurate to that of the base frequency is introduced, this continuum time translation symmetry is broken. The symmetry in time becomes discrete: the periodicity of the external signal introduces an additional time scale that breaks the continuum time symmetry.

Let us denote T_e as the period of the external signal and $\omega_e = 2\pi/T_e$ as its angular frequency. It is clear from the above, that the continuum time translation symmetry is broken: a privileged time interval is introduced in the system through the external forcing and the behaviour of the oscillatory system is not expected to be similar at T_e and at $T_e/2$. However, it is clear that at discrete times that are integer multiples m of the external period (at times $t + mT_e$) the dynamics must be invariant, i.e. the resulting equation, incorporating the external forcing, must have the following invariance

$$W \rightarrow W \exp(\mathrm{i}\omega_e T_e/n), \tag{46}$$

where n is defined from the equation $\exp(\mathrm{i}2\pi n) = \exp(\mathrm{i}\omega_e T_e)$. Of course, the CGLE satisfies this invariance since it is invariant for arbitrary phase transformations. However, the CGLE equation modified to incorporate the external forcing is no longer invariant for arbitrary phase transformations, but only for the specific phase transformation in Equation (46). In the following text we discuss the modification of the CGLE to account for the continuum time symmetry breaking.

Since the externally introduced forcing resonates with the homogeneous oscillation, this means, that we can write [21]

$$\omega_e = \frac{n}{m}(\omega_0 - v), \tag{47}$$

where n/m is an irreducible integer fraction. The parameter v, assumed to be small, expresses the deviation of the forcing from being a rational multiple of the base frequency ω_0. Replacing $T_e = 2\pi/\omega_e$ in Equation (46) we have

$$W \rightarrow W \exp(\mathrm{i}2\pi/n). \tag{48}$$

We can now modify the CGLE by a term $h(W,W^*)$ to account for this invariance and for the symmetry breaking

$$\partial_t W = W - (1 + \mathrm{i}c_2)|W|^2 W + (1 + \mathrm{i}c_1)\partial_x^2 W + h(W, W^*). \tag{49}$$

By introducing the transformation in Equation (48), we can factorise the exponential factor $\exp(\mathrm{i}2\pi/n)$ and we obtain

$$\partial_t W = W - (1 + \mathrm{i}c_2)|W|^2 W + (1 + \mathrm{i}c_1)\partial_x^2 W + h(W\exp(\mathrm{i}2\pi/n), W^*\exp(-\mathrm{i}2\pi/n))\exp(-\mathrm{i}2\pi/n). \tag{50}$$

It is to be noted that, since we have simultaneously to break phase invariance for all phase transformations like that in Equation (4), which do not correspond to the specific ones in Equation (46), the simplest form of $h(W,W^*)$ satisfying both properties with the lowest nonlinearity so that

$$h(W\exp(\mathrm{i}2\pi/n), W^*\exp(-\mathrm{i}2\pi/n))\exp(-\mathrm{i}2\pi/n) = h(W, W^*) \tag{51}$$

is

$$h(W, W^*) = \gamma_1 W + \gamma_n W^{*n-1}, \tag{52}$$

where γ_1 and γ_n are complex parameters. Since the frequency is detuned by v compared to the homogeneous oscillation of the CGLE and no damping is introduced through the forcing, it is clear that for the linear term we have $\gamma_1 = \mathrm{i}v$. The modified CGLE accounting for the external resonant forcing has thus the form

$$\partial_t W = (1 + \mathrm{i}v)W - (1 + \mathrm{i}c_2)|W|^2 W + (1 + \mathrm{i}c_1)\partial_x^2 W + \gamma_n W^{*n-1}. \tag{53}$$

This equation is known to have n different stationary solutions which correspond to phase locked states in which the oscillatory system gets entrained by the external resonant forcing [21]. We can see this by replacing $W = R\exp(\mathrm{i}\phi)$ in Equation (53) with R and ϕ both constant in space and time. We obtain

$$\begin{aligned} R - R^3 + \gamma_n R^{n-1}\cos(n\phi) &= 0, \\ vR - c_2 R^{n-1}\sin(n\phi) &= 0. \end{aligned} \tag{54}$$

Eliminating ϕ in the latter expressions gives

$$\gamma_n^2 = \frac{(R^2 - \mu)^2 + (v - c_2 R^2)^2}{R^{2(n-2)}}. \tag{55}$$

Solving the latter expression for R and inserting it in Equation (54), ϕ gives n different solutions separated by a phase increment $2\pi/n$ [21,22]. These solutions are all stable in the strong forcing limit. They are connected spatially through the so-called Ising or Bloch walls where the absolute value of the complex amplitude $|W|$ vanishes or rotates in the complex plane, respectively. While the former are static, the latter propagate through space at constant velocity

[23]. In Figure 9 and 10 the spatiotemporal evolutions of modulus and phase of the complex amplitude for the case of $n = 3$ at high coupling strength are shown. We observe that, after a transient, the spatial oscillators cluster at three different phases separated by $2\pi/3$. The walls separating the cluster domains move with a constant velocity and, therefore, they correspond to Bloch walls.

A beautiful example of experiments performed under a 2:1 external resonant forcing of the Belousov–Zhabotinsky equation is shown in Figure 11, where, besides some different kinds of standing and spiral waves, two-phase cluster domains are observed in two dimensions [24]. These results can be modelled with an externally forced CGLE like Equation (53) in two dimensions with $n = 2$.

7. From local to global through (spatially) nonlocal coupling. Generalising the CGLE

The CGLE as described above in the previous sections describes Stuart–Landau oscillators which are coupled spatially through diffusion. This is a local spatial coupling where the value of the complex amplitude $W(x,t)$ at one point x, is related to the ones in its immediate vicinity through the second spatial derivative that constitutes the diffusion operator. In nature, other forms of spatial coupling exist, however, going beyond the local coupling provided by diffusion. In electrochemical systems, for example, the electrostatic potential makes a nonlocal coupling between points on an electrode, since the electrostatic force can be felt by a long range of locations [25]. In multicomponent systems, where some species diffuse quickly, adiabatic elimination

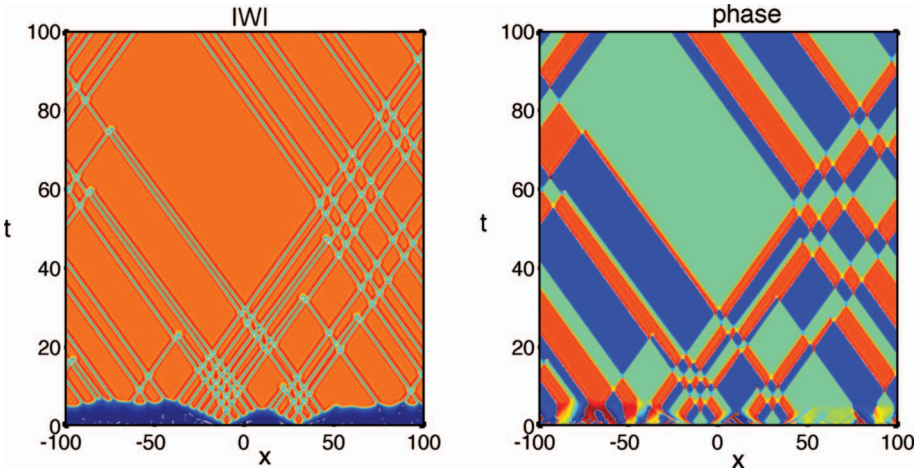

Figure 9. Spatiotemporal evolution of the absolute value $|W|$ of the complex amplitude (left) and phase (right) for the externally forced CGLE: $n = 3$, $\nu = 0$, $\gamma_n = 2.5$, $c_1 = -2.5$, $c_2 = 1$.

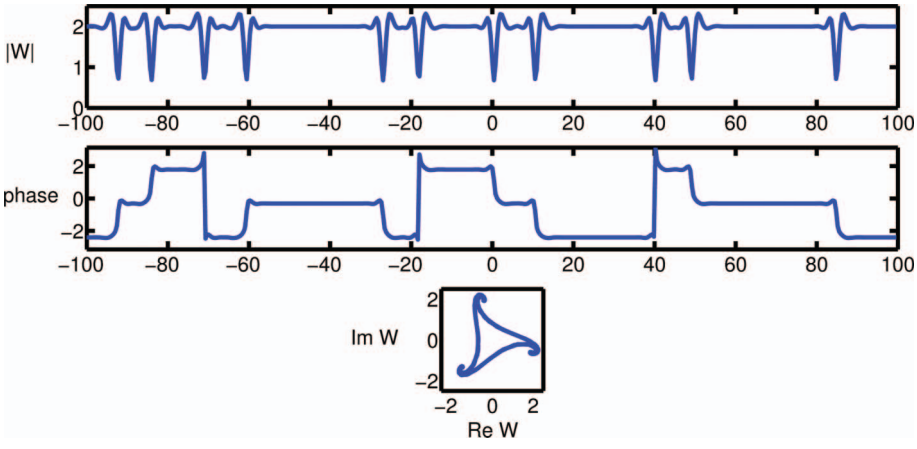

Figure 10. Spatial profiles of the modulus and phase of the complex amplitude W, and plot of W on the complex plane for the parameter values in Figure 9 at time $t = 100$.

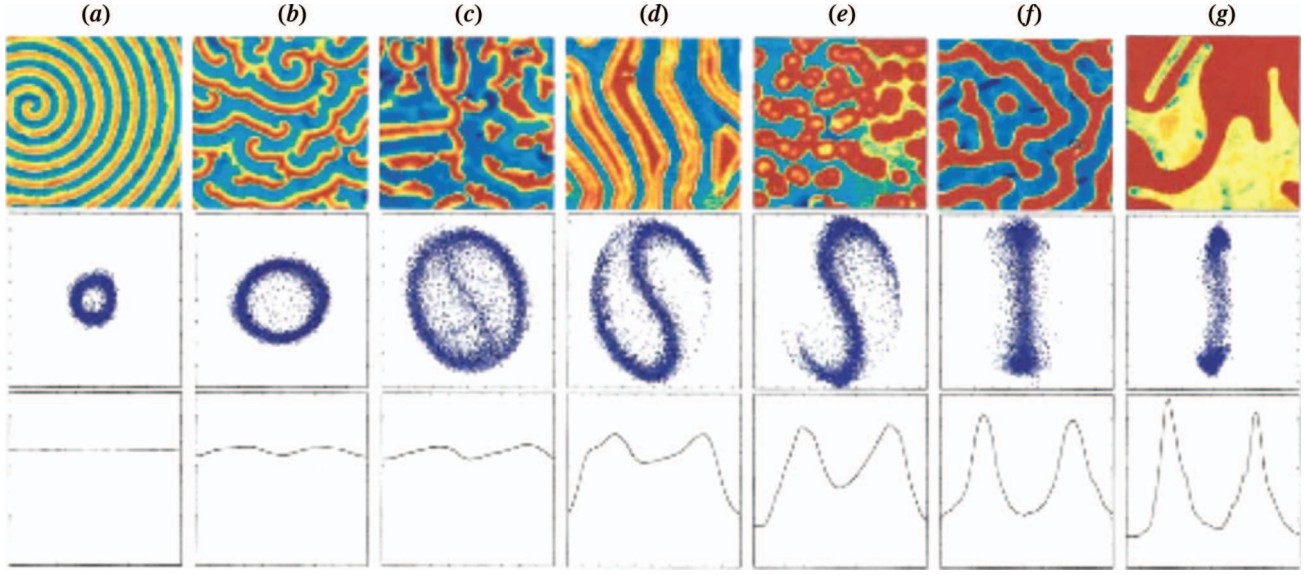

Figure 11. Different observed patterns in the periodically forced Belousov–Zhabotinsky reaction (taken from [24]), presented using a rainbow (false) colour map: (*a*) unforced rotating spiral wave, (*b*) rotating spiral wave, (*c*) mixed rotating spiral and standing wave pattern, (*d*)–(*g*) qualitatively different standing wave patterns. Patterns (*b*)–(*g*) exhibit a 2:1 resonance in the temporal power spectrum of the pattern. (middle row) The complex Fourier amplitude w for each image: the abscissa is Re w and the ordinate is Im w. (bottom row) Histograms of phase angles of all the pixels in each image. In (*g*) the apparition of two domains with opposite phase (two-phase clusters separated by an Ising wall) is observed. Reproduced figure with permission from A.L. Lin, M. Bertram, K. Martinez, H.L. Swinney, A. Ardelea, and G.F. Carey, Phys. Rev. Lett. 84 (2000), p. 4240. Copyright (2000) by the American Physical Society.

may lead to a nonlocal coupling of the remaining species [26]. Finally, a global coupling of all points in the system can be introduced by a variety of experimental means. For example, in certain surface chemical reactions, the global coupling is produced through interactions with the gas phase where rapid mixing is realised [27,28].

All forms of spatial coupling such that the resulting CGLE satisfies translation symmetry $W(x,t) \rightarrow W(x + x_0,t)$ can be summarised in a single generalised nonlocal CGLE, where the diffusion operator is replaced by an integral operator with a nonlocal kernel $H(|x-x'|)$, which depends on the distance between two points x and x'

$$\partial_t W = W - (1 + \mathrm{i}c_2)|W|^2 W + (1 + \mathrm{i}c_1) \times \int H(|x - x'|)[W(x') - W(x)]\mathrm{d}x'. \quad (56)$$

In the latter expression, the integral extends over the whole extension of the system of length L. We now list some specific forms of the kernel and give some appropriate references. First we note however that when

$$H(|x - x'|) = \delta^{(2)}(x - x'), \quad (57)$$

where $\delta(x)$ is the Dirac delta function (and (2) denotes its second derivative) the CGLE is recovered because of a well known property of the delta function

$$\int \delta^{(n)}(x - x')f(x')\,\mathrm{d}x' = (-1)^n \frac{\mathrm{d}^n f(x)}{\mathrm{d}x^n}.$$

Other forms of the integral kernel as introduced recently (after some rescalings) are

- (chemical systems under global coupling [27–31])

$$H(|x - x'|) = \delta^{(2)}(x - x') + \frac{\gamma \exp(\mathrm{i}\chi)}{L}, \quad (58)$$

  where γ and χ are real parameters. This equation was successfully employed to describe the experimentally observed turbulent patterns during catalytic CO oxidation on Pt(110) and the control of turbulence in such situations [32] (see Figure 12).
- (multicomponent systems with a fast diffusive component with rapid kinetics [26,33–35])

$$H(|x - x'|) = \frac{k}{2D^{1/2}} \exp(-|x - x'|/D^{1/2}) \quad (59)$$

  with D being the diffusion coefficient of the inactive species and k a coupling strength.

- (electrochemical systems [36,37])

$$H(|x-x'|)=\frac{\pi}{4\beta^2\sinh^2([\pi(x-x')]/2\beta)}+\frac{\delta(|x-x'|)}{\beta}, \tag{60}$$

where β is a parameter controlling the distance between the working and the counterelectrode in an electrochemical cell [38]. The equation employing this kernel was shown [36] to predict the existence of electrochemical turbulence as found in the experiments [39] (see Figure 13) and simulations [40]. Specifically, Equation (60) correctly predicts that a large coupling range β leads to a lower density of defects. This is

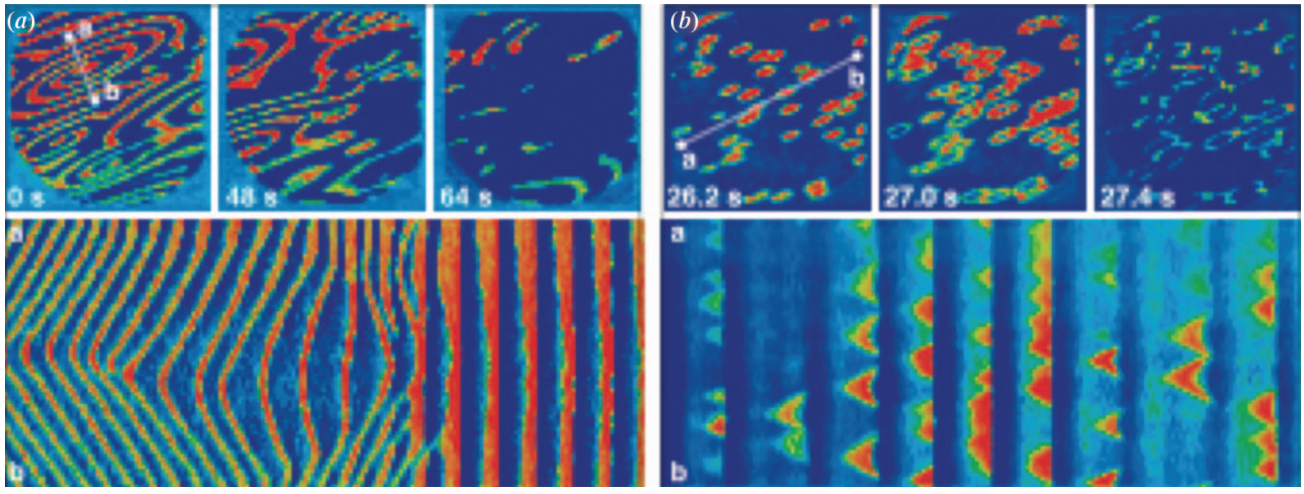

Figure 12. Experimental spatiotemporal patterns observed in experiments with global delayed feedback during the catalytic CO oxidation on Pt(110) (taken from [32]). Upper row: snapshots of the 2D dynamics; lower row: 1D cross-section indicated above versus time. (*a*) Suppression of spiral-wave turbulence; (*b*) intermittent turbulence.

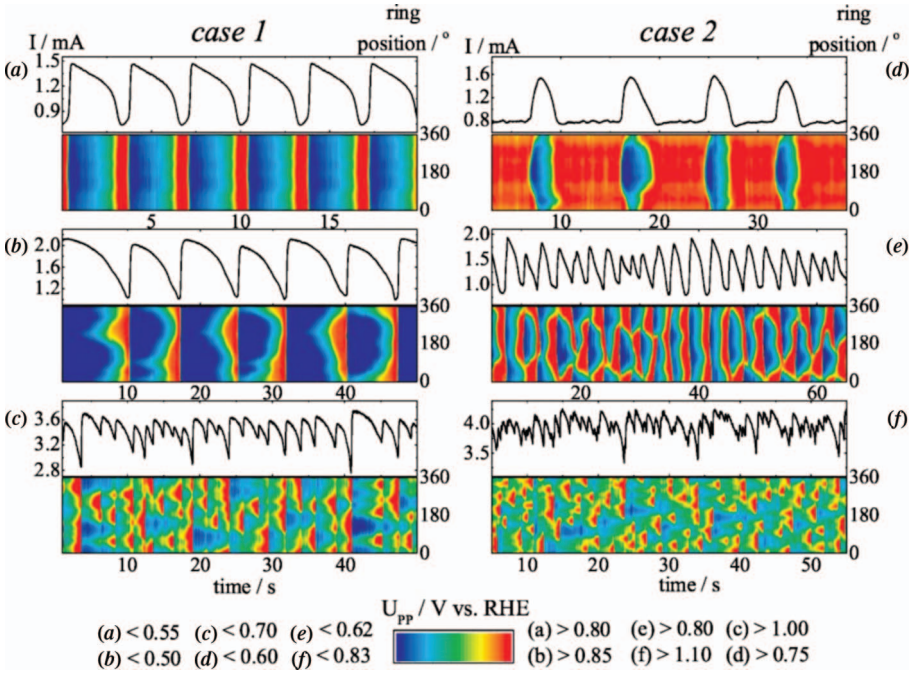

Figure 13. Experimentally observed spatiotemporal evolution of the electric current through a 1D ring electrode showing a transition to electrochemical turbulence from an homogeneous oscillatory state. Experiments denoted *case* 1 on the left were carried out at large coupling range β, while those denoted *case* 2 on the right were carried out with low β (taken from [39]). Reproduced figure with permission from H. Varela, C. Beta, A. Bonnefont, and K. Krischer, Phys. Rev. Lett. 94 (2005), 174104. Copyright (2005) by the American Physical Society.

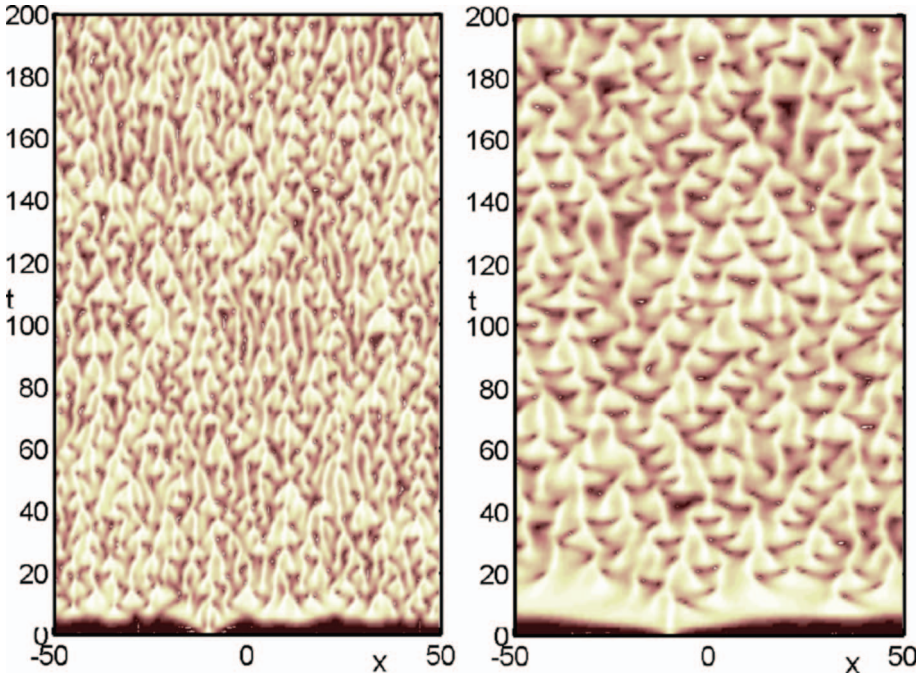

Figure 14. Spatiotemporal evolution of the modulus of the amplitude $|W|$ as calculated from Equation (56) with $H(x-x')$ given by Equation (60) for $c_1 = -1.03$, $c_2 = 2.68$, $L = 100$, and $\beta = 1$ (left) and 50 (right). Low $|W|$: dark. The figures on the right and on the left compare to Figure 13 (*c*) and (*f*), respectively (taken from [36]). Reproduced figure with permission from V. Garcia-Morales and K. Krischer, Phys. Rev. Lett. 100 (2008), 054101. Copyright (2008) by the American Physical Society.

observed in Figure 14, where the spatiotemporal evolution of $|W|$ for low and high β is plotted on the left and on the right, respectively. Equation (60) was also satisfactorily mapped to the experimental dynamics of the reduction of IO^{-4} on an Au electrode providing an accurate prediction of the onset of electrochemical turbulence on that system [36].

- (electrochemical systems under global coupling [41])

$$H(|x-x'|) = \frac{\pi}{4\beta^2 \sinh^2([\pi(x-x')]/2\beta)} + \frac{(\gamma/L) + \delta(|x-x'|)}{\beta}. \qquad (61)$$

This equation (and its version with a nonlinear global coupling [42]) describes, for example, the experimentally observed patterns in the H_2-electrooxidation reaction on a Pt ring-electrode under global coupling [43].

8. Conclusions

The CGLE describes generically many physical situations where a spatially homogeneous equilibrium state loses stability to oscillations. Besides the system length, it depends only on two parameters, and, thus, allows for the most concise discussion of pattern formation and instabilities in oscillatory systems. In this article, only the most basic solutions were discussed. Much of the knowledge about spatio-temporal disordered, chaotic states, as in the above examples of phase and defect turbulence, is due to studies of the CGLE. We would like to encourage the reader to dive further into the CGLE and discover the beauty and richness of pattern formation in oscillatory systems. The article has not discussed the mathematical technicalities of how to map an evolution equation based on physical variables and parameters to the CGLE (see, e.g. [2]). Rather, our effort has been oriented to show how the CGLE can be understood by simple symmetry considerations. Such an understanding of the CGLE may constitute, in our view, a necessary smooth bridge between undergraduate Physics and advanced treatments consistent with current research in the CGLE.

Generally, the way of comparing experimental results on oscillatory spatially extended systems to the results by the CGLE (or a version of it) is provided by the Hilbert transform of the experimental data. The Hilbert transform [44] allows one to convert an experimentally oscillating physical signal (say, an oscillating concentration of chemical species) to amplitude and phase of oscillations. Such a frame

allows for direct comparison of experiments with numerical results obtained from the CGLE. This comparison proves sometimes essential to gain an understanding and classify the experimentally observed patterns. Although strictly valid only in the close proximity of the Hopf bifurcation, in the past the CGLE was shown to give insight in pattern formation and underlying bifurcations even in situations where the system was rather far away from the Hopf bifurcation.

Acknowledgements

The authors gratefully acknowledge Kathrin Kostorz and Lennart Schmidt for their comments on the manuscript. Financial support from the cluster of excellence Nanosystems Initiative Munich (NIM) is gratefully acknowledged. V.G.-M. acknowledges also financial support from the Technische Universität München – Institute for Advanced Study, funded by the German Excellence Initiative.

Notes on contributors

Vladimir Garcia-Morales received his Ph.D. in Physics from the University of Valencia (Spain) in 2005, winning the Prize for Excellent Achievements during the doctorate. After a short DAAD Fellowship at the Technische Universität München in year 2006, he moved in 2007 to the latter university where he started working in collaboration with Katharina Krischer in fundamental aspects of nonlinear dynamics of electrochemical systems. In 2010 he was awarded a Carl von Linde Junior Fellowship from the Institute of Advanced Study of the Technische Universität München, a position that he currently holds. His scientific interests include: advanced methods of Mathematical Physics, the theoretical study of complex, chaotic and nonlinear phenomena, Nonequilibrium Statistical Mechanics and Nanothermodynamics.

Katharina Krischer did her graduate studies at the Fritz-Haber-Institut of the Max-Planck-Society in Berlin in the department of Prof. Ertl on Oscillations and Instabilities in two surface reactions. After receiving her Ph.D. in 1990, she moved as a postdoc to the Princeton University and returned to the Fritz-Haber Institut in 1992, first as a research assistance and later she became a group leader. Since 2002, she has been a professor at the Physics Department at the Technical University of Munich. Her research focuses on nonequilibrium chemical physics. Katharina Krischer received several prizes, among them the De Gruyter award of the Berlin-Brandenburg Academy of Sciences and the Otto-Hahn-Medaille of the Max-Planck Society.

References

[1] C. Beta, A.S. Mikhailov, H.H. Rotermund, and G. Ertl, *Defect-mediated turbulence in a catalytic surface reaction*, Europhys. Lett. 75 (2006), p. 868.
[2] Kuramoto, Y. *Chemical Oscillations, Waves and Turbulence*, 1st ed., Springer-Verlag, Berlin, 1984.
[3] A.C. Newell and J.A. Whitehead, *Finite bandwidth, finite amplitude convection*, J. Fluid. Mech. 38 (1969), p. 279.
[4] K. Stewartson and J.T. Stuart, *A non-linear instability theory for a wave system in plane Poiseuille flow*, J. Fluid. Mech. 48 (1971), p. 529.
[5] M.C. Cross and P.C. Hohenberg, *Pattern formation outside of equilibrium*, Rev. Mod. Phys. 65 (1993), p. 851.
[6] A.C. Newell, T. Passot, and J. Lega, *Order parameter equations for patterns*, Ann. Rev. Fluid Mech. 25 (1993), p. 399.
[7] L.M. Pismen, *Vortices in Nonlinear Fields*, Oxford Science Publications, Oxford, UK, 1999.
[8] T. Bohr, M.H. Jensen, G. Paladin, and A. Vulpiani, *Dynamical Systems Approach to Turbulence*, Cambridge University Press, Cambridge, UK, 1998.
[9] G. Dangelmayr and L. Kramer, *Mathematical approaches to pattern formation,* in *Evolution of Spontaneous Structures in Dissipative Continuous Systems*, F.H. Busse and S.C. Müller, eds., Springer, New York, 1998, pp. 1–85.
[10] I.S. Aranson and L. Kramer, *The world of the complex Ginzburg–Landau equation*, Rev. Mod. Phys. 74 (2002), p. 99.
[11] P. Manneville, *Dissipative Structures and Weak Turbulence*, Academic Press, San Diego, CA, 1990.
[12] W. van Saarloos, *The complex Ginzburg–Landau equation for beginners,* in *Spatiotemporal Patterns in Nonequilibrium Complex Systems*, Santa Fe Institute Series in the Sciences of Complexity, Addison-Wesley, Reading, 1993.
[13] M. van Hecke, P.C. Hohenberg, and W. van Saarloos, *Amplitude equations for pattern forming systems*, in *Fundamental Problems in Statistical Mechanics VIII*, H. van Beijren and M.H. Ernst, eds., North-Holland, Amsterdam, 1994, p. 245.
[14] G. Nicolis, *Introduction to Nonlinear Science*, Cambridge University Press, Cambridge, UK, 1995.
[15] D. Walgraaf, *Spatio-temporal Pattern Formation*, Springer-Verlag, New York, 1997.
[16] B.I. Shraiman, A. Pumir, W. van Saarloos, P.C. Hohenberg, H. Chate, and M. Holen, *Spatiotemporal chaos in the one-dimensional complex Ginzburg–Landau equation*, Physica D 57 (1992), p. 241.
[17] E. Bodenschatz, W. Pesch, and G. Ahlers, *Recent developments in Raleigh–Bénard convection*, Annu. Rev. Fluid. Mech. 32 (2000), p. 709.
[18] Q. Ouyang and J.M. Flesselles, *Transition from spirals to defect turbulence driven by a convective instability*, Nature 379 (1996), p. 143.
[19] F. Siegert and C. Weijer, *Digital image processing of optical density wave propagation in* Dictyostelium discoideum *and analysis of the effects of caffeine and ammonia*, J. Cell. Sci. 93 (1989), p. 325.
[20] J.M. Gambaudo, *Perturbation of a Hopf bifurcation by an external time periodic forcing*, J. Diff. Eqs. 57 (1985), p. 172.
[21] P. Coullet and K. Emilsson, *Strong resonances of spatially distributed systems: a laboratory to study patterns and defects*, Physica D 61 1992, p. 119.
[22] A.L. Lin, A. Hagberg, A. Ardelea, M. Bertram, H.L. Swinney, and E. Meron, *Four-phase patterns in forced oscillatory systems*, Phys. Rev. E 62 (2000), p. 3790.
[23] P. Coullet, J. Lega, B. Houchmanzadeh, and J. Lajzerowicz, *Breaking chirality in nonequilibrium systems*, Phys. Rev. Lett. 65 (1990), p. 1352.
[24] A.L. Lin, M. Bertram, K. Martinez, H.L. Swinney, A. Ardelea, and G.F. Carey, *Resonant phase patterns in a reaction-diffusion system*, Phys. Rev. Lett. 84 (2000), p. 4240.

[25] K. Krischer, *Nonlinear dynamics in electrochemical systems*, in *Advances in Electrochemical Sciences and Engineering*, D.M. Kolb and R.C. Alkire, eds., Wiley-VCH, Weinheim, 2003, p. 89.
[26] D. Tanaka and Y. Kuramoto, *Complex Ginzburg–Landau equation with nonlocal coupling*, Phys. Rev. E 68 (2003), 026219.
[27] F. Mertens, R. Imbihl, and A. Mikhailov, *Breakdown of global coupling in oscillatory chemical reactions*, J. Chem. Phys. 99 (1993), p. 8668.
[28] F. Mertens, R. Imbihl, and A. Mikhailov, *Turbulence and standing waves in oscillatory chemical reactions with global coupling*, J. Chem. Phys. 101 (1994), p. 9903.
[29] M. Falcke and H. Engel, *Pattern formation during the CO oxidation on Pt(110) surfaces under global coupling*, J. Chem. Phys. 101 (1994), p. 6255.
[30] M. Falcke, H. Engel, and M. Neufeld, *Cluster formation, standing waves and stripe patterns in oscillatory media with local and global coupling*, Phys. Rev. E 52 (1995), p. 763.
[31] D. Battogtokh and A. Mikhailov, *Controlling turbulence in the complex Ginzburg–Landau equation*, Physica D 90 (1996), p. 84.
[32] M. Kim, M. Bertram, M. Pollmann, A. von Oertzen, A.S. Mikhailov, H.H. Rotermund, and G. Ertl, *Controlling chemical turbulence by global dealyed feedback: pattern formation in catalytic CO oxidation on Pt(110)*, Science 292 (2001), p. 1357.
[33] Y. Kuramoto, *Scalin behavior of turbulent oscillators with non-local interaction*, Prog. Theor. Phys. 94 (1995), p. 321.
[34] Y. Kuramoto, *Phase- and Center-manifold reductions for large populations of coupled oscillators with application to non-locally coupled systems*, Int. J. Bifurcation Chaos Appl. Sci. Eng. 7 (1997), p. 789.
[35] Y. Kuramoto, D. Battogtokh, and H. Nakao, *Multi-affine chemical turbulence*, Phys. Rev. Lett. 81 (1998), p. 3543.
[36] V. Garcia-Morales and K. Krischer, *Nonlocal complex Ginzburg–Landau equation for electrochemical systems*, Phys. Rev. Lett. 100 (2008), 054101.
[37] V. Garcia-Morales, R.W. Hölzel, and K. Krischer, *Coherent structures emerging from turbulence in the nonlocal complex Ginzburg–Landau equation*, Phys. Rev. E 78 (2008), 026215.
[38] J. Christoph and M. Eiswirth, *Theory of electrochemical pattern formation*, Chaos 12 (2002), p. 215.
[39] H. Varela, C. Beta, A. Bonnefont, and K. Krischer, *Transitions to electrochemical turbulence*, Phys. Rev. Lett. 94 (2005), 174104.
[40] N. Mazouz, *Wellen und stationäre Strukturen in elektrochemischen Systemen*, Ph.D. thesis, Freie Universität Berlin, 1999.
[41] V. Garcia-Morales and K. Krischer, *Normal-form approach to spatiotemporal pattern formation in globally coupled electrochemical systems*, Phys. Rev. E 78 (2008), 057201.
[42] V. Garcia-Morales, A. Orlov, and K. Krischer, *Subharmonic phase clusters in the complex Ginzburg–Landau equation with nonlinear global coupling*, Phys. Rev. E 82 (2010), 065202(R).
[43] H. Varela, C. Beta, A. Bonnefont, and K. Krischer, *A hierarchy of global coupling induced cluster patterns during the oscillatory H_2-electrooxidation reaction on a Pt ring-electrode*, Phys. Chem. Chem. Phys. 7 (2005), p. 2429.
[44] A. Pikovsky, M. Rosenblum, and J. Kurths, *Synchronization: A Universal Concept in Nonlinear Sciences*, Cambridge University Press, Cambridge, UK, 2001.